UNCL

SECURITY C

# AD-A197 709 OCUMENTATION PAGE

④

| 1a. REPORT NA | 1b. RESTRICTIVE MARKINGS NA |
|---|---|
| 2a. SECURITY CLASSIFICATION AUTHORITY NA | 3. DISTRIBUTION/AVAILABILITY OF REPORT Distribution Unlimited; Approved for Public Release |
| 2b. DECLASSIFICATION/DOWNGRADING SCHEDULE NA | |

| 4. PERFORMING ORGANIZATION REPORT NUMBER(S) INDU/DC/GMH/TR-88-30 | 5. MONITORING ORGANIZATION REPORT NUMBER(S) NA |
|---|---|

| 6a. NAME OF PERFORMING ORGANIZATION Indiana University | 6b. OFFICE SYMBOL (If applicable) NA | 7a. NAME OF MONITORING ORGANIZATION ONR |
|---|---|---|

| 6c. ADDRESS (City, State, and ZIP Code) Department of Chemistry Bloomington, IN 47405 | 7b. ADDRESS (City, State, and ZIP Code) 800 N. Quincy Street Arlington, VA 22217 |
|---|---|

| 8a. NAME OF FUNDING/SPONSORING ORGANIZATION | 8b. OFFICE SYMBOL (If applicable) | 9. PROCUREMENT INSTRUMENT IDENTIFICATION NUMBER Contract N00014-86-K-0366 |
|---|---|---|

| 8c. ADDRESS (City, State, and ZIP Code) | 10. SOURCE OF FUNDING NUMBERS | | | |
|---|---|---|---|---|
| | PROGRAM ELEMENT NO. | PROJECT NO. | TASK NO. R&T Code 4134006 | WORK UNIT ACCESSION NO |

11. TITLE (Include Security Classification)

Characterization of the Microwave-Induced Plasma as a Detector for Supercritical Fluid Chromatography

12 PERSONAL AUTHOR(S)  Leonard J. Galante, Mark Selby, Debra R. Luffer, Gary M. Hieftje, and Milos Novotny

| 13a. TYPE OF REPORT Technical | 13b. TIME COVERED FROM _____ TO _____ | 14. DATE OF REPORT (Year, Month, Day) July 11, 1988 | 15. PAGE COUNT 42 |
|---|---|---|---|

16. SUPPLEMENTARY NOTATION

Accepted for publication in Analytical Chemistry

| 17. COSATI CODES | | | 18. SUBJECT TERMS (Continue on reverse if necessary and identify by block number) |
|---|---|---|---|
| FIELD | GROUP | SUB-GROUP | Supercritical Fluid Chromatography, Nonmetal Detection, Spectroscopic Detector, Speciation, Sulfur Detection. |
| | | | |
| | | | |

19. ABSTRACT (Continue on reverse if necessary and identify by block number)

A microwave-induced plasma (MIP) sustained in helium is evaluated as an element-selective detector for capillary supercritical fluid chromatography (SFC). The plasma source, a surface-microwave-induced plasma (surfatron), is described. Optimal plasma conditions including viewing position, helium flow rate, and applied microwave power are discussed for sulfur emission in the near-infrared spectral region. In addition, the effects of two common mobile phases ($CO_2$ and $N_2O$) on plasma stability, sensitivity, and spectral background from 200 nm to 1100 nm are assessed. Although the plasma was evaluated principally for use with SFC, much of the discussion is relevant to its application as a gas chromatographic detector.

| 20 DISTRIBUTION/AVAILABILITY OF ABSTRACT ☒ UNCLASSIFIED/UNLIMITED ☐ SAME AS RPT ☐ DTIC USERS | 21 ABSTRACT SECURITY CLASSIFICATION Distribution Unlimited |
|---|---|
| 22a. NAME OF RESPONSIBLE INDIVIDUAL Gary M. Hieftje | 22b TELEPHONE (Include Area Code) (812) 335-2189 | 22c OFFICE SYMBOL |

**DD FORM 1473,** 84 MAR          83 APR edition may be used until exhausted          SECURITY CLASSIFICATION OF THIS PAGE
All other editions are obsolete

UNCLASSIFIED

OFFICE OF NAVAL RESEARCH

Contract N14-86-K-0366

R&T Code 4134006

TECHNICAL REPORT NO. 30

CHARACTERIZATION OF THE MICROWAVE-INDUCED PLASMA

AS A DETECTOR FOR SUPERCRITICAL FLUID CHROMATOGRAPHY

by

Leonard J. Galante, Mark Selby, Debra R. Luffer,
Gary M. Hieftje, and Milos Novotny

Accepted for Publication

in

ANALYTICAL CHEMISTRY

Indiana University
Department of Chemistry
Bloomington, Indiana 47405

| Accession For | |
| --- | --- |
| NTIS GRA&I | ☒ |
| DTIC TAB | ☐ |
| Unannounced | ☐ |
| Justification | |
| By | |
| Distribution/ | |
| Availability Codes | |
| Dist | Avail and/or Special |
| A-1 | |

11 July 1988

## INTRODUCTION

Capillary gas chromatography (GC) and capillary liquid chromatography (LC) possess inherent liabilities that make them unsuitable for many types of separations. The former is ultimately restricted by the limited volatility and thermal lability of many organic compounds. The latter is restricted by the limited number of theoretical plates that it can provide in a practical analysis time and by the unavailability of sensitive universal or element-selective detectors (1).

Capillary supercritical fluid chromatography (SFC) has been recognized as an attractive complementary method for compounds that are not amenable to separation by GC or LC. For example, a supercritical fluid mobile phase can solvate large, relatively involatile molecules at temperatures that are significantly lower than those required in GC. SFC can also provide efficient separations in much shorter analysis times than LC because of the lower mobile phase viscosities of supercritical fluids and greater solute diffusivities (2).

The column effluent in SFC, unlike that in LC, is typically a gas at atmospheric pressure. Consequently, SFC is inherently compatible with many of the sensitive universal detectors employed in gas chromatography (1, 3). To date, several of these detection arrangements including SFC/FID (4), SFC/MS (5, 6) and SFC/FTIR (7, 8) have been explored. Several selective detectors such as the thermionic (9) and dual flame photometric (10) detectors have also been coupled to a supercritical fluid chromatograph.

Plasma atomic-emission sources such as the inductively coupled plasma (ICP) (11) or microwave-induced plasma (MIP) (12-14) are also

attractive detectors for chromatography because of their inherent selectivity and multielement detection capability. In addition, imperfect chromatographic resolution is less troublesome with plasma detectors because of their elemental selectivity.

The MIP has been shown to be particularly useful as an element-specific detector for GC (15-18). Fortunately, many of the desirable features of the MIP make it suitable as a detector for capillary SFC as well; in general, these plasmas are small, relatively inexpensive, and compatible with gaseous-sample introduction. The helium-sustained MIP is particularly attractive because both nonmetals and metals can be sensitively detected (14). In addition, the MIP can perform as a universal detector for hydrocarbons by tuning the monochromator to a hydrogen or carbon emission wavelength.

In this paper, a helium microwave-induced plasma is explored as an element-selective detector for capillary SFC. The plasma was supported by a surface-wave structure termed a surfatron (19), similar to that used earlier for GC detection (20-22). The effects of the mobile phase ($CO_2$ and $N_2O$) on plasma stability, sensitivity, and spectral background from 200 nm to 1100 nm were assessed, and the optimal plasma operating conditions were ascertained for sulfur emission at 921.3 nm. Sulfur was chosen because of its prevalence in biochemical and environmental samples.

## EXPERIMENTAL

### Instrumentation

A schematic diagram of the surfatron source and the optical system appears in Figure 1. Each component is described below.

The surfatron used for these studies was constructed of brass and is similar to the design of Abdallah et al. (23). Details concerning the construction, operation, and tuning of our device have been described elsewhere (24).

The surfatron was powered by a microwave generator (Microtron 200 Mark III, 0-200 W, 2450 ± 25 MHz, Electro-Medical Supplies Ltd., Wantage Oxfordshire, England), which was modified to incorporate an isolator consisting of a 3-port circulator (type 6SI27, 0.2 db insertion loss, 20 db isolation, 350 W maximum, Junction Devices, Westlake Village, CA) and a matched load (model 8135 coaxial resistor, 50 ohms, 150 W maximum, Bird Electronic Corporation, Cleveland, OH). The isolator increases the stability of the magnetron under load and protects the unit from excessive reflected power. Forward and reflected power levels were measured with the meters on the generator. A 1.5-m length of coaxial cable (Belden, #8242, RG-9/U, Richmond, IN) was employed as a transmission line between the surfatron and the generator.

The plasma was viewed axially (end-on configuration) and, unless indicated otherwise, in the radial center of the discharge tube. For measurements in the UV-visible spectral region, a quartz lens (44-mm d., 97-mm focal length) imaged the plasma onto the entrance slit (10 $\mu$m) of the monochromator (model EU-700, 0.35-m focal length, Heath Co., Benton Harbor, MI) with a magnification of 2.10. The grating was ruled at 1200 grooves/mm and blazed at 250 nm. The photomultiplier tube (1P28, Hamamatsu Corp., Middlesex, NJ) was mounted in a non-cooled housing (model 50B, Pacific Photometric Instruments, Emeryville, CA) and biased at -1000 V with a high-voltage supply (Keithley Instruments, Inc., Cleveland, OH).

For measurements in the near-infrared spectral region, a glass lens (24-mm d., 71-mm focal length) imaged the plasma onto the entrance slit (10 $\mu$m) of the monochromator with a magnification of 1.25. A long-pass filter (red glass, model 51512, Oriel, Stratford, CT) blocked second-order radiation. The grating was ruled at 600 grooves/mm and blazed at 1000 nm. The photomultiplier tube (model 7102, Hamamatsu) was biased at -1250 V with a high-voltage supply (model 1121A, EG & G Princeton Applied Research, Princeton, NJ) and mounted in a thermoelectrically cooled housing (models 7102/117 and TE104RF-002, Products for Research, Inc., Danvers, MA); tap water was employed as the heat-exchange medium.

The output current of the PMT was measured with a picoammeter (model 414S, Keithley Instruments) and received by a strip-chart recorder (model SR-204, Heath Co.). The time constant of the data-collection system was 0.3 sec.

The plasma was ordinarily sustained inside a 6-mm o.d. x 4-mm i.d. fused-silica tube (William A. Sales Ltd., Wheeling, IL) in high-purity grade helium (Air Products, Tamaqua, PA). Spectra were obtained with ultra-pure carrier-grade helium, technical-grade nitrous oxide, and C. P. grade carbon dioxide (Air Products, Allentown, PA), all supplied by cylinders. The helium flow rate was regulated by a rotameter (model 602, Matheson, Joliet, IL).

## Procedures

With the tuning adjustments of our surfatron set to nearly optimal positions (24), the plasma can be initiated by touching the inside of the discharge tube with a length of tungsten wire. Alternatively, the plasma can be ignited with a short burst from a Tesla coil. Immediately

after the plasma was ignited, the tuning adjustments were set to zero
reflected power.

Low flow rates (0.1-1.0 mL/min) of either $CO_2$ or $N_2O$ were mixed
with the helium support gas and introduced into the plasma to
investigate their effect on spectral background and nonmetal emission
sensitivity. These gases were added ahead of the discharge tube through
a Nupro® fine-metering valve (series S-SS1, 1/16 in. Swagelok® with
vernier handle, Nupro, Co., Willoughby, OH). The flow rate of the added
gas was measured with a bubble meter constructed from a 2.0-mL graduated
pipette.

Carbon disulfide (analytical-reagent grade, Mallinckrodt, Inc.,
Paris, KY) or thiophene (Eastman Kodak, Co., Rochester, NY) vapor was used
to evaluate the optimal operating conditons for the detection of
volatilized sulfur-containing compounds in the surfatron-sustained
plasma. These vapors were introduced continuously into the plasma by
sweeping the headspace above a small volume of the liquid with a small
flow of helium (<1.0 mL/min), which was subsequently mixed with the
helium support gas prior to entering the discharge tube. The liquid was
contained in a small glass tube immersed in a dry ice/acetone bath to
reduce its vapor pressure. A schematic diagram of the headspace-vapor-
sampling apparatus is shown in reference 25. In these experiments, the
amount of sulfur entering the plasma was estimated to be below
50 ng/sec, and the background intensity and background noise were
determined at a wavelength adjacent to the sulfur spectral peak.

## RESULTS AND DISCUSSION

### Effect of the SFC Mobile Phase on Plasma Shape and Appearance

Most microwave plasmas possess limitations that make them incompatible or difficult to use with many sample-introduction methods. For example, they are very susceptible to impedance changes and are easily detuned by foreign material because they are sustained in a resonant cavity (13). In addition, plasma stability and excitation are perturbed by large amounts of solute or solvent (12, 16). A conventional MIP can usually withstand the injection of only approximately 17 $\mu$g/sec or 3-5 $\mu$g (absolute) of foreign material before signal stability is seriously affected; however, this upper limit depends somewhat on the cavity type and operating conditions (12).

In contrast to resonant-cavity devices, the surfatron sustains an annular plasma in helium by surface waves that are launched along the discharge tube. Accordingly, the plasma is brightest near the walls of the discharge tube where the radial electric-field is greatest, but is weaker and more diffuse at the center of the discharge tube (24). These features give the plasma greater resistance to detuning effects caused by solvent or solute loading (24, 26). The surfatron-sustained plasma is therefore well-suited for SFC detection where relatively large amounts (3-120 $\mu$g/sec) of $CO_2$ exit the column at typical mobile phase flow rates (1-10 $\mu$L/min) and densities (0.2-0.7 g/mL).

The surfatron-sustained plasma can operate with $CO_2$ and $N_2O$ concentrations that are within the above range. However, the appearance and shape of the plasma depend strongly upon the amount of the added molecular gas and on the applied power. At 100 W and a helium flow rate of 120 mL/min, the plasma's appearance is unaffected by either $N_2O$ or

$CO_2$ added at rates below 0.2 mL/min (atmospheric pressure) (6 $\mu$g/sec).

However, as the flow rate of added gas approaches 0.6 mL/min (18 $\mu$g/sec),

the hole in the center of the plasma widens and becomes more prominent;

the plasma also becomes less vibrant in appearance. The plasma becomes

asymmetrical at a $CO_2$ or $N_2O$ flow rate of 0.75 mL/min (23 $\mu$g/sec). To

sustain a stable, more robust and symmetrical plasma at higher $CO_2$ and

$N_2O$ flow rates, more power is required. For example, 150 W is needed to

sustain a symmetrical plasma at a $CO_2$ or $N_2O$ flow rate of 1.2 mL/min (36

$\mu$g/sec). The plasma is almost completely extinguished when the added-gas

flow rate approaches 18 mL/min (15% of the support gas (v/v)) or

540 $\mu$g/sec.

**Effect of the SFC Mobile Phase on Spectral Background**

In the absence of an SFC mobile phase, the spectral background from

the surfatron-sustained plasma in the UV-visible (Figure 2) and the

near-infrared (Figure 3) spectral regions consists largely of atomic

emission from He, Si, O, C, N, and H (27). These elements are

introduced into the plasma by the support gas, from the discharge tube,

and with entrained air. Hydrogen atom emission at 656.3 nm (Figure 3)

makes the plasma appear pink instead of yellow as expected for a plasma

sustained in pure helium (28). Background emission arises also from

molecular species because of incomplete atomization and recombination.

The principal molecular bands (29) are summarized in Table I. As shown

in later figures, the intensities of many of these background features

decrease considerably when either $CO_2$ or $N_2O$ are introduced into the

plasma.

<u>Carbon-Dioxide-Doped Plasma</u>.   Carbon dioxide has a dramatic effect on spectral background, particularly in the UV-visible region (Figure 4) where several intense molecular bands exist for CO, $CO^+$, CN, and $C_2$ (cf. Table I).   These background features could preclude or interfere with the sensitive determination of many elements.   For example, the $C_2$ bands between 540 and 565 nm (Table I) coincide with the sulfur ion lines at 542.9, 543.3, 545.4, 560.6, and 564.0 nm that are often used with the MIP for sulfur determinations in the UV-visible region (30). Even with a non-carbon-containing mobile phase, the spectral interference from $C_2$ at these sulfur wavelengths would be severe in SFC because of the large molecular weights of typical solutes.   These sulfur ion lines are even less useful when the surfatron source is used because their emission intensities are relatively weak.

Emission from $C_2$ between 450 and 550 nm makes the plasma appear blue-green under the conditions used to obtain Figure 4.   However, changes in $CO_2$ concentration, helium flow rate, and microwave power dramatically influence the color of the plasma.   When the support gas contains about 0.1% $CO_2$ (v/v) and the microwave power is 100 W, the plasma annulus is bright green.   As the $CO_2$ concentration increases, the annulus becomes more bluish, dullish, and diffuse, and the hole in the center of the plasma widens.   Near the 1% $CO_2$ level and 100 W of applied power, the plasma annulus becomes dark blue and asymmetrical, but becomes brighter, thicker, greener, and more symmetrical as the power increases.

As shown in Figure 5, the near-infrared region appears more attractive than the UV visible for SFC separations that require $CO_2$. This region is not only relatively free of intense molecular bands, it

offers better sensitivity for certain nonmetals, including O, N, Cl, Br, and particularly sulfur (25, 30). The sulfur atom lines at 921.3, 922.8, and 923.8 nm are strongest in the surfatron-sustained plasma and have relative intensities of 100, 71, and 42, respectively. These relative intensities are similar to those observed by Freeman and Hieftje from the He-MIP sustained in a $TM_{010}$ (Beenakker) cavity (30) and by Hubert et al. (31) from an MIP sustained in a surfatron.

Nitrous-Oxide-Doped Plasma. Nitrous oxide is another commonly used nonpolar mobile phase in SFC. It has a critical point that is very similar to that of $CO_2$ (32), and can separate many of the same compounds. It would also be more useful than $CO_2$ for SFC/MIP determinations that are based on carbon emission.

As shown in Figure 6, nitrous oxide produces stronger background spectral features than $CO_2$ over much of the UV-visible region. The principal molecular bands are listed in Table I. Again, the near-infrared region (Figure 7) appears more attractive for SFC analyses because of the absence of intense molecular bands.

As shown in Figure 8A, $N_2O$ is a somewhat more desirable SFC mobile phase than $CO_2$ for sulfur determinations because it produces a cleaner background spectrum at 921.3 nm, the most sensitive sulfur line. Carbon dioxide produces a moderately intense CN band that is coincident with the three most intense sulfur lines that exist between 921 nm and 924 nm (Figure 8B and Table I).

Optimal Plasma Conditions for the Determination of Sulfur in Volatilized Organic Compounds

Spatial Position. The effect of horizontal viewing position in the plasma on sulfur (*) and background emission intensity (◎) at 100 W for

$CS_2$ vapor appears in Figure 9. Sulfur emission intensity is clearly greater by a factor of at least 1.5 and 1.9 near the walls of the discharge tube (at 1.7 mm and -1.7 mm, respectively) than at the radial center (0 mm). The shape of the emission map is not surprising, considering the plasma's annular shape. The support gas (helium) and other nonmetals, such as Cl and I, produce similar emission profiles in the surfatron when they are introduced into the plasma as gases (26).

In contrast, background intensity (Figure 9) and background noise are relatively independent of viewing position. Accordingly, the signal-to-background (S/B) and signal-to-background noise (S/N) profiles are similar to the sulfur intensity profile of Figure 9. However, as elaborated below, the viewing position for optimal S/B and S/N appears to depend on microwave power.

Effect of Applied Microwave Power. As shown in Figure 10, sulfur intensity first increases as the microwave power is raised, irrespective of the chosen viewing position (0 mm or 1.7 mm). However, the intensity levels off above an applied power of 150 W. In contrast, S/B and S/N (Figure 11) are maximal at 75-100 W and decrease as power goes up. The decline in S/B and S/N with increasing power is much greater at the plasma annulus (1.7 mm) than at the center of the discharge (0 mm). Accordingly, the central viewing position is preferred at higher powers.

Effect of Helium Flow Rate. The effect of helium support-gas flow rate on emission intensity for sulfur introduced at a constant rate as $CS_2$ headspace vapor is shown in Figure 12. At very low helium flow rates, the plasma is not very robust and S(I) emission intensity is weak. Sulfur intensity increases rapidly as the flow rate is raised and becomes strongest at about 120 mL/min. The intensity drops at higher

flow rates because the hole in the center of the plasma increases and the width of the annulus decreases. The drop in intensity at high flow rates might be caused also by a decrease in analyte residence time. Flow rate affected S/N and S/B in a similar manner. A similar trend and the same optimum flow rate (Figure 12) were observed for carbon (present as a carbon impurity and at a constant concentration in the helium support gas).

Optimal Plasma Conditions for SFC Separations. Earlier work suggests that the optimal helium flow rate and viewing position depend dramatically upon the method of sample introduction and the element of interest (26). In chromatographic applications, optimal conditions will naturally depend also upon the nature of the interface between the chromatographic column and the plasma. In a companion study (33), we show that the optimal helium flow rate is somewhat higher than 120 mL/min for sulfur compounds actually separated by SFC and detected with the surfatron-sustained plasma. This finding has been attributed to our interface design (33) and the increased dilution of the SFC solvent ($CO_2$) by the plasma support gas.

## Effect of the SFC Mobile Phase on Sulfur Sensitivity

Gases such as $H_2$, $O_2$, and $N_2$ are often used as dopants for gas chromatography and mixed with the helium support gas of the MIP in small amounts (0.1-1% v/v) to reduce carbon deposition on the walls of the discharge tube (12, 16, 17). However, these dopant gases are known also to quench the helium plasma and to cause a corresponding decrease in elemental emission for several nonmetals, including S and the halogens

(14). Chlorine ion and fluorine atom intensity can be affected at dopant concentrations as low as 0.01% and 0.001%, respectively (28).

It is evident from the background spectra in Figures 2 through 7 that $CO_2$ and $N_2O$ also affect excitation in the surfatron plasma. These gases quench portions of the background continuum and decrease molecular and atomic emission from a variety of species. The effect of these gases on He atomic emission at 1083.0 nm is compared in Figure 13. Here, the gases were added to the helium support gas (120 mL/min) at rates from 0.1 to 1.0 mL/min (3 to 30 $\mu$g/sec). The most dramatic decrease in helium emission intensity (about 90%) occurs when the gases are added at a rate of 3 $\mu$g/sec, which is the lowest rate anticipated in SFC. Emission intensity decreases more gradually at higher mass flow rates.

The effect of added argon, also shown in Figure 13, is less severe than that of the molecular gases. These data suggest that a supercritical fluid composed of a noble gas might be desirable for SFC/MIP applications. A monoatomic gas would also produce a lower spectral background. Unfortunately, only xenon has an acceptable critical temperature and pressure (32) for SFC, and it is rather expensive.

Figure 14 shows the effect of added $CO_2$ on background and sulfur emission intensity at 921.29 nm and at a plasma power of 100 W. The background intensity (dotted curve in Figure 14) at first gradually increases with $CO_2$ concentration and reaches a maximum at 0.1-0.3 mL/min (3-9 $\mu$g/sec) of added $CO_2$. The initial increase can be attributed to CN emission (Table I). However, background intensity decreases at higher concentrations because of plasma quenching. As shown in Figure 14

(solid curve), sulfur intensity is quenched by added $CO_2$ and decreases continuously over the studied $CO_2$ concentration range. Similar trends were observed for data collected at a microwave power of 200 W.

Signal-to-background ratios measured at 100 and 200 W of applied power appear in Figure 15. At both power settings, the signal-to-background ratio for sulfur decreases by a factor of about five when C.2 mL/min (6 $\mu$g/sec) of $CO_2$ is mixed with the plasma support gas. The ratios remain relatively constant at higher $CO_2$ concentrations. Importantly, it appears that sensitivity cannot be improved by increasing the applied microwave power.

## CONCLUSIONS

The surfatron-sustained microwave-induced plasma has been s'.own to be a viable element-selective detector for supercritical fluid chromatography that operates at relatively low powers and helium flow rates. These studies have shown that the near-infrared spectral region appears to be advantageous for SFC determinations because of greater freedom from molecular background features caused by the mobile phase. Although the mobile-phase gas will diminish sensitivity somewhat, a companion study (33) has shown that detection limits are in the low pg/sec range. Such sensitivity is suitable for many applications.

# CREDIT

## Literature Cited

1  Novotny, M. HRC & CC **1986**, <u>9</u>, 137-144.

2  Novotny, M.; Springston, S. R.; Peaden, P. A.; Fjeldsted, J. C.; Lee, M. L. Anal. Chem. **1981**, <u>53</u>, 407A-414A.

3  Chester, T. L. J. Chromatogr. Sci. **1986**, <u>24</u>, 226-229.

4  White, C. M.; Houck, R. K. HRC & CC **1986**, <u>9</u>, 4-17.

5  Wright, B. W.; Kalinoski, H. T.; Udseth, H. R.; Smith, R. D. HRC & CC **1986**, <u>9</u>, 145-153.

6  Lee, E. D.; Henion, J. D. HRC & CC **1986**, <u>9</u>, 172-174.

7  Pentoney, S. L., Jr.; Shafer, K. H.; Griffiths, P. R. J. Chromatogr. Sci. **1986**, <u>24</u>, 230-235.

8  Pentoney, S. L., Jr.; Shafer, K. H.; Griffiths, P. R.; Fuoco R. HRC & CC **1986**, <u>9</u>, 168-171.

9  West, W. R.; Lee, M. L. HRC & CC **1986**, <u>9</u>, 161-167.

10 Markides, K. E.; Lee, E. D.; Bolick, R.; Lee, M. L. Anal. Chem. **1986**, <u>58</u>, 740-743.

11 Hieftje, G. M. In Analytical Atomic Spectroscopy; Holcombe, J. A., Ed.; Wiley, in press, 1987.

12 Zander, A. T.; Hieftje, G. M. Appl. Spectrosc. **1981**, <u>35</u>, 357-371.

13 Matousek, J. P.; Orr, B. J.; Selby, M. Prog. Anal. At. Spectrosc. **1984**, <u>7</u>, 275-314.

14 Van Dalen, J.P.J.; de Lezenne Coulander, P. A.; de Galan, L. Anal. Chim. Acta **1977**, <u>94</u>, 1-19.

15 Mohamad, A. H.; Caruso, J. A. In Advances in Chromatography; Giddings, J. C.; Grushka, E.; Brown, P. R., Eds; Marcel Dekker:  New York, 1987; Vol. 26, Chapter 5.

16 Risby, T. H.; Talmi, Y. CRC Crit. Rev. Anal. Chem. 1983, 14, 231-265.

17 Beenakker, C.I.M. Spectrochim. Acta, Part B 1977, 32, 173-187.

18 Lisk, D. J.; Bache, C. A. Anal. Chem. 1967, 39, 786-789.

19 Hubert, J.; Moisan, M.; Ricard, A. Spectrochim. Acta, Part B 1979, 34, 1-10.

20 Moisan, M.; Ferreira, C. M.; Hajlaoui, Y.; Henry, D.; Hubert, J.; Pantel, R.; Ricard, A.; Zakrzewski, Z. Rev. Phys. Appl. 1982, 17, 707-727.

21 Chevrier, G.; Hanai, T.; Tran, K. C.; Hubert, J. Can. J. Chem. 1982, 60, 898-903.

22 Hanai, T.; Coulombe, S.; Moisan, M.; Hubert, J. In Developments in Atomic Plasma Spectrochemical Analysis; Barnes, R. M., Ed.; John Wiley and Sons: Chichester, 1981; pp 337-344.

23 Abdallah, M. H.; Coulombe, S.; Mermet, J. M.; Hubert, J. Spectrochim. Acta, Part B 1982, 37, 583-592.

24 Selby, M.; Hieftje, G. M. Spectrochim. Acta, Part B 1987, 42, 285-298.

25 Freeman, J. E.; Hieftje, G. M. Spectrochim. Acta, Part B 1985, 40, 653-664.

26 Selby, M.; Rezaaiyaan, R.; Hieftje, G. M. Appl. Spectrosc. 1987, 41, 749-761.

27 Massachusetts Institute of Technology Wavelength Tables, Vol. 2: Wavelengths by Element; Phelps, F. M., III, preparer; MIT Press: Cambridge, MA, 1982.

28 Koirtyohann, S. R. Anal. Chem. 1983, 55, 374-376.

29 Pearse, R.W.B.; Gaydon, A. G. The Identification of Molecular Spectra, 4th ed.; Wiley: New York, 1976.

30 Freeman, J. E.; Hieftje, G. M. *Spectrochim*. *Acta*, *Part* *B* 1985, 40, 475-492.

31 Hubert, J.; Tra, H. V.; Tran, K. C.; Baudais, F. L. *Appl*. *Spectrosc*. 1986 40, 759-766.

32 *CRC* *Handbook* *of* *Chemistry* *and* *Physics*, 60th ed.; Weast, R. C., Ed.; CRC Press: Boca Raton, Florida, 1979.

33 Luffer, D. R.; Galante, L. J.; David, P. A.; Novotny, M.; Hieftje, G. M. *Anal*. *Chem*., submitted for publication.

Table I. Major Sources of Interfering Band Emission in the Helium Surfatron-Sustained Plasma.[a]

| Molecular Species | Band Origin | Wavelength (nm) | Relative Intensity of Feature |
|---|---|---|---|
| **A.  Helium Plasma** | | | |
| NO | (1,0) | 215.5,  214.9 | weak |
| | (0,0) | 226.9,  226.3 | weak |
| | (0,1) | 237.0,  236.3 | weak |
| | (0,2) | 247.9,  247.1 | weak |
| | (0,3) | 259.6,  258.8 | weak |
| OH | (1,0) | 281.1 | moderate |
| | (0,0) | 306.4 | very strong |
| NH | (0,0) | 336.0 | very strong |
| | (1,1) | 337.0 | very strong |
| $N_2$ (2nd positive) | (0,1) | 357.7 | moderate |
| | (1,3) | 375.5 | weak |
| | (0,2) | 380.5 | weak |
| $N_2^+$ | (0,0) | 391.4 | moderate |
| | (0,1) | 427.8 | weak |
| $N_2$ (1st positive) | (1,0) | 891.2 | weak |
| | (2,0) | 775.3 | weak |
| | (3,1) | 762.6 | weak |
| | (4,2) | 750.4 | weak |
| | (5,3) | 738.7 | weak |
| **B.  $CO_2$-Doped Plasma** | | | |
| CO | (1,8) | 200.6 | moderate |
| | (5,11) | 201.2 | moderate |
| | (2,9) | 202.6 | moderate |
| | (3,10) | 204.6 | moderate |
| | (4,11) | 206.8 | moderate |
| | (5,12) | 209.0 | moderate |
| $CO^+$ | (1,0) | 211.2 | moderate |
| | (2,1) | 213.8 | moderate |
| | (0,0) | 219.0 | strong |
| | (1,1) | 221.5 | moderate |
| | (0,1) | 230.0 | strong |
| | (1,2) | 232.5 | moderate |
| | (0,2) | 241.9 | moderate |
| | (1,3) | 244.6 | moderate |

| Molecular Species | Band Origin | Wavelength (nm) | Relative Intensity of Feature |
|---|---|---|---|
| | (1,4) | 257.8 | weak |
| | (2,5) | 260.7 | weak |
| | (3,6) | 263.9 | weak |
| OH | (1,0) | 281.1 | weak |
| | (0,0) | 306.4 | strong |
| NH | (0,0) | 336.0 | weak |
| | (1,1) | 337.0 | weak |
| CN | (3,2) | 358.4 | |
| (Violet | (2,1) | 358.6 | strong |
| System) | (1,0) | 359.0 | |
| | (4,4) | 385.1 | |
| | (3,3) | 385.5 | |
| | (2,2) | 386.2 | very strong |
| | (1,1) | 387.1 | |
| | (0,0) | 388.3 | very strong |
| | (5,6) | 415.2 | |
| | (4,5) | 415.8 | |
| | (3,4) | 416.8 | moderate |
| | (2,3) | 418.1 | |
| | (1,2) | 419.7 | |
| | (0,1) | 421.6 | |
| $C_2$ | (4,2) | 436.5 | |
| (Swan | (3,1) | 437.1 | weak |
| System) | (2,0) | 438.3 | |
| | (5,4) | 467.9 | |
| | (4,3) | 468.5 | |
| | (3,2) | 469.8 | |
| | (2,1) | 471.5 | |
| | (1,0) | 473.7 | strong |
| | (1,1) | 512.9 | strong |
| | (0,0) | 516.5 | very strong |
| | (4,5) | 547.0 | |
| | (3,4) | 550.2 | |
| | (2,3) | 554.1 | weak |
| | (1,2) | 558.6 | moderate |
| | (0,1) | 563.6 | |
| CN | (3,0) | 692.6 | |
| (red | (4,1) | 708.9 | weak |
| system) | (5,2) | 728.3 | |
| | (2,0) | 787.3 | |
| | (3,1) | 806.7 | weak |
| | (4,2) | 827.1 | |
| | (1,0) | 914.1 | moderate |
| | (2,1) | 938.1 | |

| Molecular Species | Band Origin | Wavelength (nm) | Relative Intensity of Feature |
|---|---|---|---|
| **C.  N₂O-Doped Plasma** | | | |
| NO | (2,0) | 205.3, 204.8 | weak |
| | (1,0) | 215.5, 214.9 | moderate |
| | (0,0) | 226.9, 226.3 | moderate |
| | (0,1) | 237.0, 236.3 | strong |
| | (0,2) | 247.9, 247.1 | strong |
| | (1,4) | 255.9, 255.0 | weak |
| | (0,3) | 259.6, 258.8 | moderate |
| | (1,5) | 268.0, 267.1 | weak |
| | (0,4) | 272.2, 271.3 | weak |
| | (1,6) | 281.0, 280.1 | weak |
| | (0,5) | 286.0, 285.0 | weak |
| $N_2$ | (4,2) | 295.3 | |
| (2nd | (3,1) | 296.2 | very strong |
| positive) | (2,0) | 297.7 | |
| | (4,3) | 310.4 | |
| | (3,2) | 311.7 | very strong |
| | (2,1) | 313.6 | |
| | (1,0) | 315.9 | |
| | (4,4) | 326.8 | |
| | (3,3) | 328.5 | |
| | (0,0) | 337.1 | very strong |
| | (1,2) | 353.7 | very strong |
| | (0,1) | 357.7 | |
| | (3,5) | 367.2 | |
| | (2,4) | 371.1 | very strong |
| | (1,3) | 375.5 | |
| | (0,2) | 380.5 | |
| | (2,5) | 394.3 | moderate |
| | (1,4) | 399.8 | moderate |
| | (0,3) | 405.9 | moderate |
| $N_2{}^+$ | (4,4) | 381.8 | |
| (1st | (3,3) | 383.5 | |
| Negative | (2,2) | 385.8 | |
| System) | (1,1) | 388.4 | |
| | (0,0) | 391.4 | very strong |
| | (4,5) | 414.1 | |
| | (3,4) | 416.7 | |
| | (2,3) | 419.9 | moderate |
| | (1,2) | 423.7 | |
| | (0,1) | 427.8 | |

| Molecular Species | Band Origin | Wavelength (nm) | Relative Intensity of Feature |
|---|---|---|---|
| $N_2$ | (7,4) | 654.5 | |
| (1st | (6,3) | 662.4 | weak |
| Positive | (5,2) | 670.5 | |
| System) | (4,1) | 678.9 | |
| | (5,3) | 738.7 | |
| | (4,2) | 750.4 | weak |
| | (3,1) | 762.6 | |
| | (2,0) | 775.3 | |
| | (2,1) | 872.2 | moderate |
| | (1,0) | 891.2 | |
| | (0,0) | 1051.0 | weak |

[a]Reference 29 was used to identify molecular bands.

## FIGURE CAPTIONS

Figure 1.    Schematic diagram of the surfatron source and optical system.

Figure 2.    Background spectrum of the helium-sustained surfatron plasma
in the UV-visible spectral region without added $CO_2$ or $N_2O$.
Helium flow rate, 120 mL/min. Microwave power, 100 W.    Full
scale: 10 $\mu A$. Many of the line intensities are off scale so
that weaker ones can be seen.

Figure 3.    Background spectrum of the helium-sustained surfatron plasma in
the near-infrared spectral region without added $CO_2$ or $N_2O$.
Helium flow rate, 120 mL/min. Microwave power, 100 W.   Full
Scale: 30 nA. Many of the line intensities are off scale so
that weaker ones can be seen.

Figure 4.    Background spectrum of the plasma in the UV-visible region with
$CO_2$ added to the support gas at a rate of 0.16 mL/min
(5 $\mu g/sec$). Other conditions are identical to those of
Figure 2.

Figure 5.    Background spectrum of the plasma in the near-infrared
region with $CO_2$ added to the support gas at a rate of 5
$\mu g/sec$. Other conditions are identical to those of Figure 3.

Figure 6.    Background spectrum of the plasma in the UV-visible region
with $N_2O$ added to the support gas at a rate of 5 $\mu g/sec$.
Other conditions are identical to those of Figure 2.

Figure 7.   Background spectrum of the plasma in the near-infrared

region with $N_2O$ added to the support gas at a rate of 5

$\mu g/sec$. Other conditions are identical to those of Figure

3.

Figure 8.   Background spectra from 895-925 nm with  A) $N_2O$ and  B) $CO_2$

added at a flow rate of 5 $\mu g/sec$ each.  The wavelengths of

the most intense S(I) and Cl(I) lines within the near-

infrared region are marked in both spectra.  Full scale: 10

nA.  Other conditions are identical to those of Figure 3.

Figure 9.   The effect of spatial viewing position on background (◎) and

S(I) intensity (*) at 921.29 nm for $CS_2$ headspace vapor.

The image of the plasma was moved horizontally across the

entrance slit of the monochromator, so that the emission was

integrated over the entire height of the plasma image.

Helium flow rate, 250 mL/min.  Microwave power, 100 W.

Figure 10.  The effect of microwave power on S(I) intensity at 921.29 nm

in the radial center of the plasma (*) and 1.7 mm from the

radial center (◎).  Sulfur source, $CS_2$ headspace vapor.

Helium flow rate, 250 mL/min.

Figure 11.  The effect of microwave power on sulfur signal-to-background

noise ratio in the radial center of the plasma (*) and 1.7

mm from the radial center (◎).  Others conditions are

identical to those of Figure 10.

Figure 12.   The effect of helium flow rate on S(I) intensity for $CS_2$

headspace vapor at 921.29 nm (*) and C(I) intensity (from a

helium impurity) at 909.48 nm (⊙).   The carbon intensities

have been multiplied by 25.  Microwave power, 100 W.


Figure 13.   The effect of $CO_2$ (solid curve), $N_2O$ (dotted curve), and Ar

(dashed and dotted curve) on He(I) emission at 1083.0 nm

when the gases are added to the support gas at flow rates of

0.1-1.0 mL/min (3-30 $\mu$g/sec).   Helium flow rate, 120 mL/min.

Microwave power, 100 W.


Figure 14.   The effect of added $CO_2$ on sulfur (—*—) and background

emission intensity (···*···) for $CS_2$ (introduced as headspace

vapor).   Helium flow rate, 120 mL/min.   Microwave power, 100 W.

Wavelength, 921.29 nm.


Figure 15.   The effect of added $CO_2$ on sulfur signal-to-background

ratio at 100 W (—*—) and 200 W (··⊙··).   Other conditions
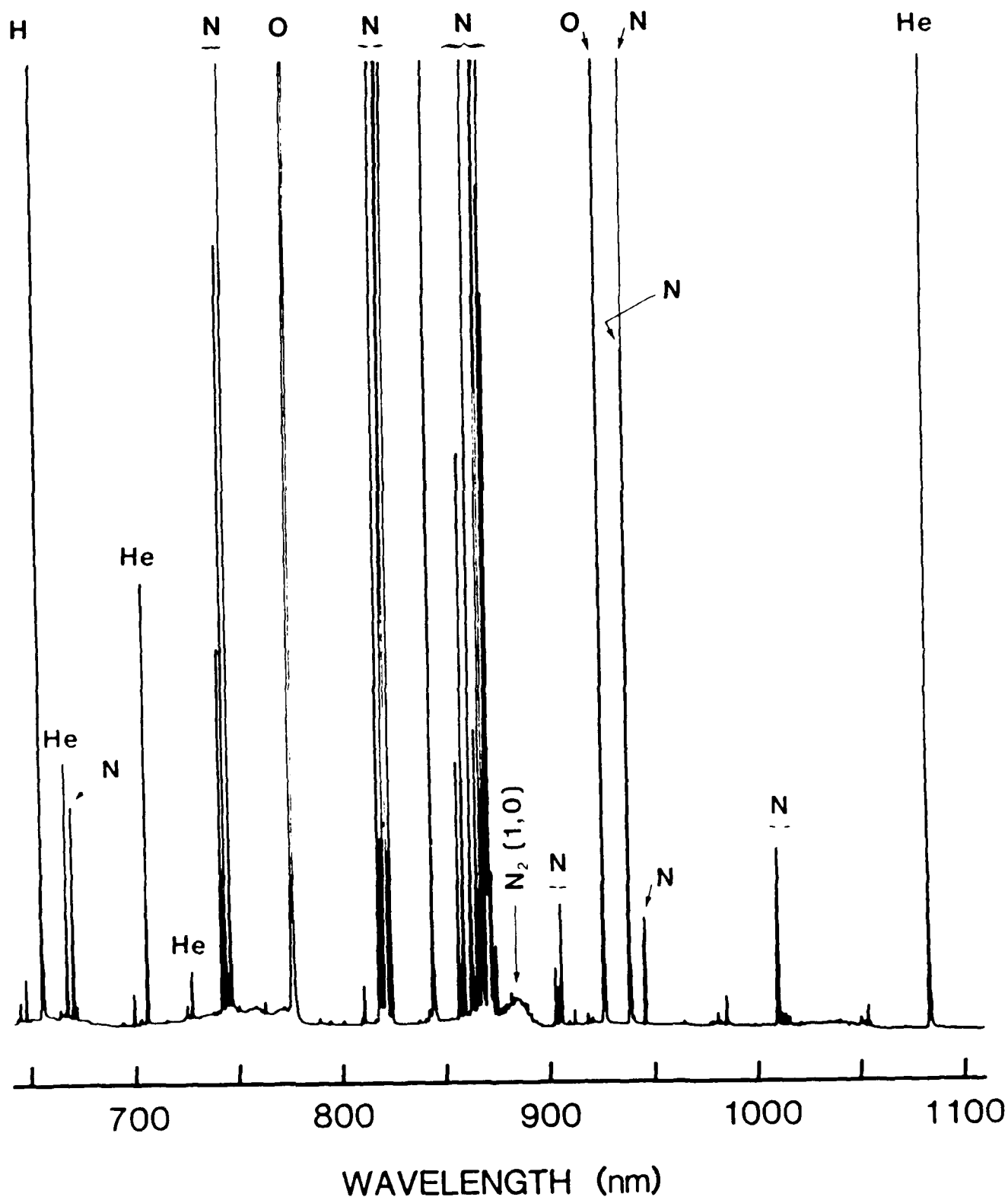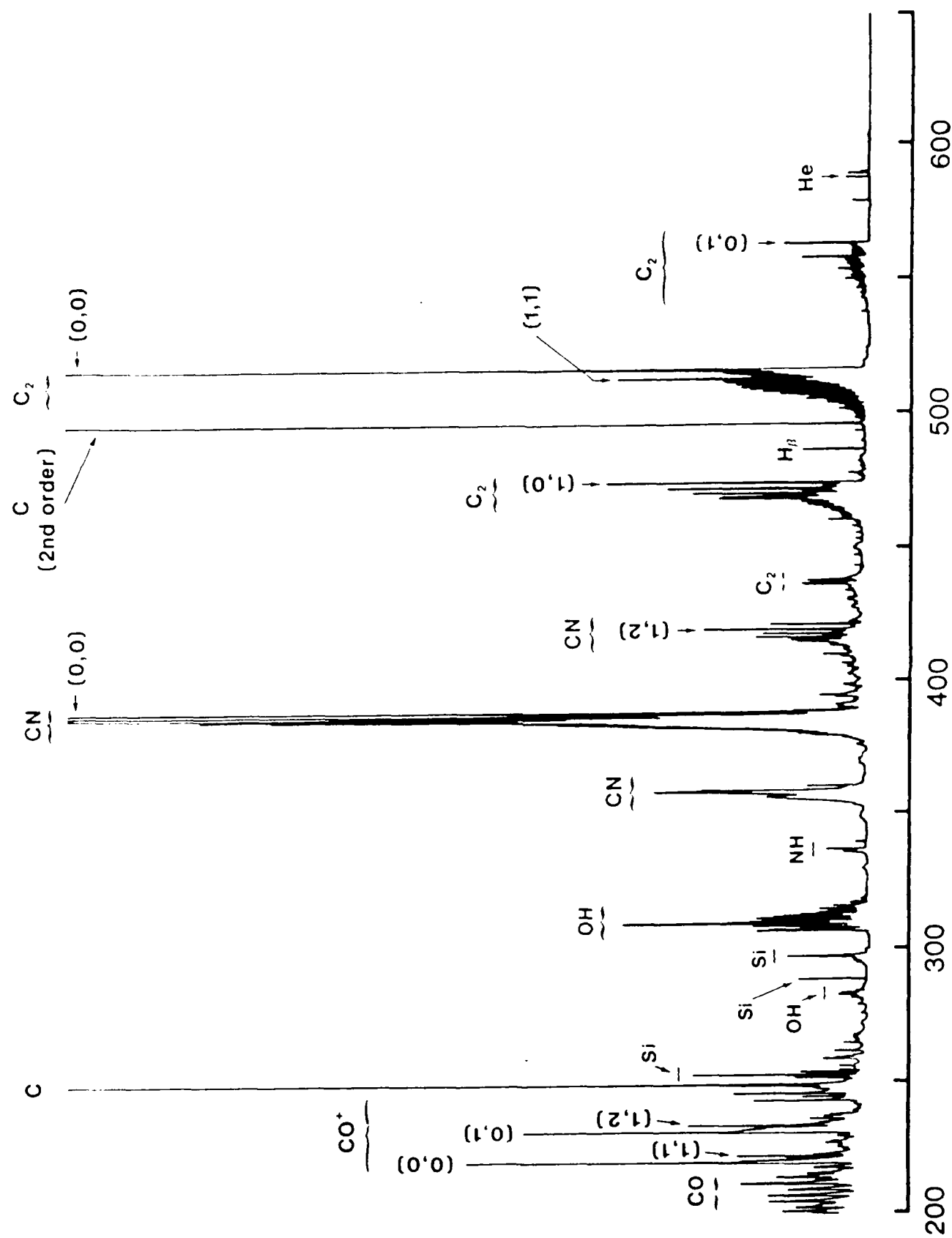
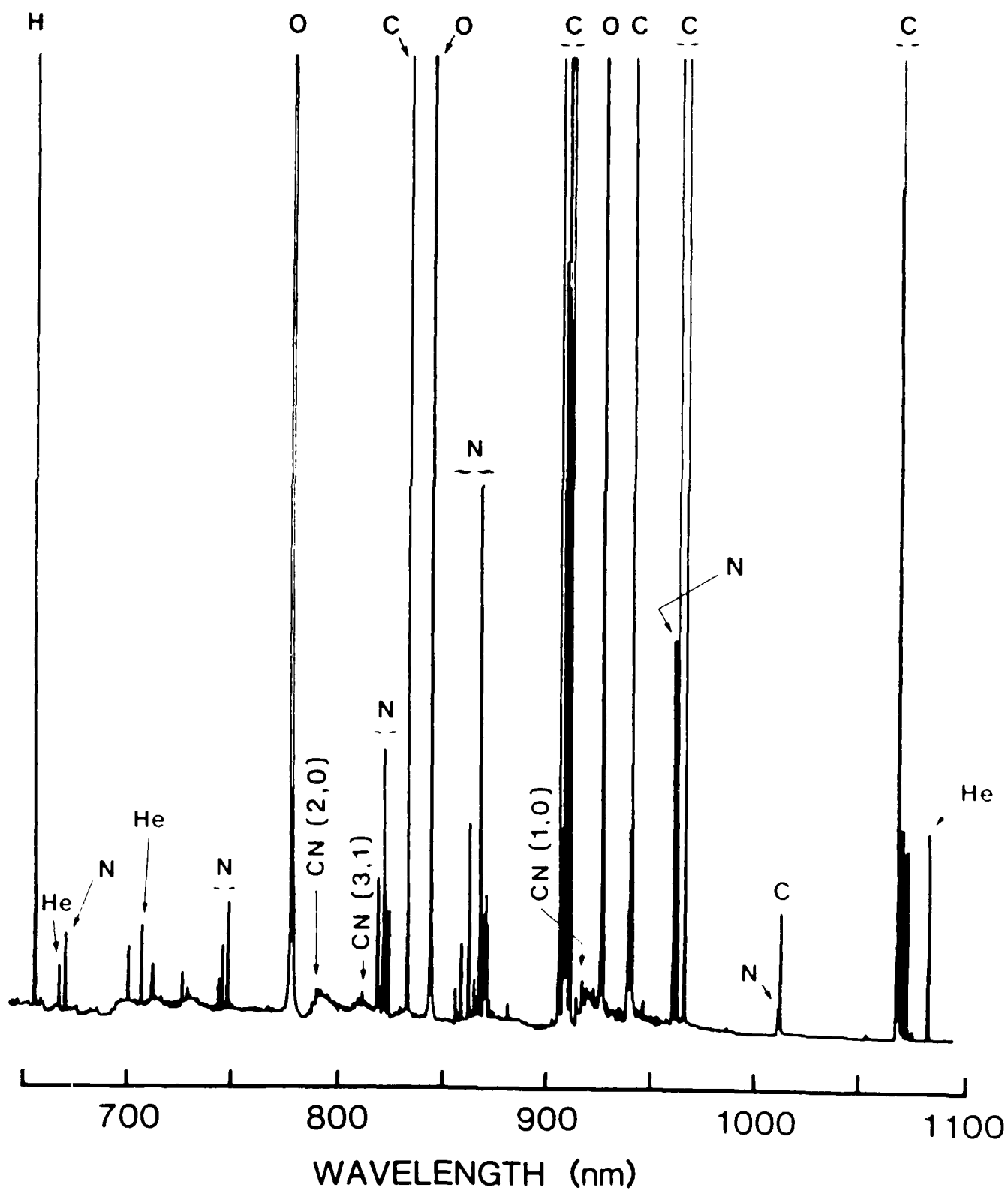are identical to those of Figure 14.

Fig. 1

Fig. 1

WAVELENGTH (nm)

Fig 3

WAVELENGTH (nm)

Figure showing emission spectrum with wavelength (nm) on horizontal axis from 200 to 600 nm, with labeled spectral features including CO, CO⁺, Si, OH, NH, CN, C₂, Hβ, He, and C.

Labels visible in the figure:
- C
- CN, (0,0)
- C₂, (0,0)
- C (2nd order)
- C₂, (1,1)
- C₂, (0,1)
- He
- Hβ
- C₂ {(1,0)}
- C₂
- CN {(1,2)}
- CN
- NH
- OH
- Si, Si
- OH
- Si
- CO⁺ {(0,0), (0,1), (1,1), (1,2)}
- CO

WAVELENGTH (nm)
200, 300, 400, 500, 600

Fig. 5

H    O    C    O    C O C C    C

N

N

He
CN (2,0)
He    N
He    N    CN (3,1)    N    CN (1,0)    N    C    He

700    800    900    1000    1100

WAVELENGTH (nm)

Fig. 6

Fig. 1

WAVELENGTH (nm)

A. N₂O

FULL SCALE

O { 926.09 nm
    926.27 nm →
    926.60 nm

N 906.05 nm →

N 902.89 nm →

N { 904.59 nm
    904.99 nm

Cl 912.11 nm

S 921.29 nm

N { 918.45 nm
    918.78 nm

N { 920.78 nm
    920.80 nm

DARK CURRENT

895   905   915   925

WAVELENGTH (nm)

B. CO₂

C 904.57 nm →

C { 906.14 nm
    906.25 nm

C 911.18 nm

C { 907.83 nm
    908.85 nm
    909.48 nm

Cl 912.11 nm

S 921.29 nm

CN
Red System

895   905   915   925

WAVELENGTH (nm)

Fig 3

RELATIVE INTENSITY

HORIZONTAL POSITION (mm)

Fig. 6

RELATIVE INTENSITY

MICROWAVE POWER (W)

Figure

Fig.

RELATIVE INTENSITY

HELIUM FLOW RATE (mL/min)

×25

RELATIVE INTENSITY

FLOW RATE OF ADDED GAS (mL/min)

$N_2O$

$CO_2$

Ar

Fig. 3

FLOW RATE OF ADDED CO₂ (mL/min)

FLOW RATE OF ADDED CO₂ (mL/min)

SIGNAL/BACKGROUND

Fig. 15

TECHNICAL REPORT DISTRIBUTION LIST, GEN

| | No. Copies | | No. Copies |
|---|---|---|---|
| Office of Naval Research<br>Attn: Code 1113<br>800 N. Quincy Street<br>Arlington, Virginia 22217-5000 | 2 | Dr. David Young<br>Code 334<br>NORDA<br>NSTL, Mississippi 39529 | 1 |
| Dr. Bernard Douda<br>Naval Weapons Support Center<br>Code 50C<br>Crane, Indiana 47522-5050 | 1 | Naval Weapons Center<br>Attn: Dr. Ron Atkins<br>Chemistry Division<br>China Lake, California 93555 | 1 |
| Naval Civil Engineering Laboratory<br>Attn: Dr. R. W. Drisko, Code L52<br>Port Hueneme, California 93401 | 1 | Scientific Advisor<br>Commandant of the Marine Corps<br>Code RD-1<br>Washington, D.C. 20380 | 1 |
| Defense Technical Information Center<br>Building 5, Cameron Station<br>Alexandria, Virginia 22314 | 12<br>high<br>quality | U.S. Army Research Office<br>Attn: CRD-AA-IP<br>P.O. Box 12211<br>Research Triangle Park, NC 27709 | 1 |
| DTNSRDC<br>Attn: Dr. H. Singerman<br>Applied Chemistry Division<br>Annapolis, Maryland 21401 | 1 | Mr. John Boyle<br>Materials Branch<br>Naval Ship Engineering Center<br>Philadelphia, Pennsylvania 19112 | 1 |
| Dr. William Tolles<br>Superintendent<br>Chemistry Division, Code 6100<br>Naval Research Laboratory<br>Washington, D.C. 20375-5000 | 1 | Naval Ocean Systems Center<br>Attn: Dr. S. Yamamoto<br>Marine Sciences Division<br>San Diego, California 91232 | 1 |